Bioorganic & Medicinal Chemistry Vol. 1, No. 2, pp. 125-140, 1993
Printed in Great Britain

0968-0896/93 $6.00 + .00

Iron(II)/Hydroperoxide (Fenton Reagent)-induced Activation of Dioxygen for (A) the Direct Ketonization of Methylenic Carbon and (B) the Dioxygenation of *cis*-Stilbene

Chan Kang, Chad Redman, Veronica Cepak and Donald T. Sawyer*
Department of Chemistry, Texas A & M University, College Station, TX 77843

(*Received* 1 *March* 1993; *accepted* 5 *April* 1993)

Abstract–Several iron complexes [$Fe^{II}(PA)_2$ (PA = picolinate), $Fe^{II}(bpy)_2^{2+}$, $Fe^{II}(OPPh_3)_4^{2+}$, $Fe^{II}(MeCN)_4^{2+}$, $(Cl_8TPP)Fe^{II}(py)_2$ (Cl_8TPP = tetrakis(2,6-dichlorophenyl)porphyrin), and $Fe^{III}Cl_3$] in combination with R'OOH (R'=H, *t*-Bu) catalytically activate O_2 to oxygenate hydrocarbons {e.g., *c*-C_6H_{12}→*c*-$C_6H_{10}(O)$ [9 O_2 turnovers per $Fe^{II}(PA)_2$ or $Fe^{II}(bpy)_2^{2+}$, and 13 per $(Cl_8TPP)Fe^{II}(py)_2$]; $PhCH_2CH_3$→$PhC(O)CH_3$ (up to 25 O_2 turnovers per $Fe^{II}L_x$); *c*-C_6H_{10}→*c*-$C_6H_8(O)$ (up to 9 O_2 turnovers per $Fe^{II}L_x$); $PhCH(Me)_2$→PhC(O)Me, $Ph(Me)_2COH$, and Ph(Me)C=CH_2 (up to 5 O_2 turnovers per $Fe^{II}L_x$); and *cis*-PhCH=CHPh→2PhCH(O) (up to 2 O_2 turnovers per FeL_x)}. With large R'OOH/FeL_x ratios spontaneous decomposition occurs to give free O_2 that is incorporated into the substrates. The product profiles for the various $Fe^{II}L_x$/R'OOH, O_2/RH systems and their electrochemical characterization during steady-state turnover confirm that the first-formed intermediate is a one-to-one R'OOH/$Fe^{II}L_x$ adduct {e.g., $[(PA)_2Fe^{II}OOR' + pyH^+]$ (**1**)} (Fenton reagent), which reacts with (a) excess $Fe^{II}(PA)_2$ to give $(PA)_2Fe^{III}OR'$, (b) excess *c*-C_6H_{12} to give (*c*-C_6H_{11})py {kinetic isotope effect, [KIE] = $k_{c\text{-}C_6H_{12}}/k_{c\text{-}C_6D_{12}}$, 4.6 with *t*-BuOOH and 1.7 with HOOH}, (c) excess R'OOH to give $[(PA)_2Fe^{IV}(OH)(OOR')]$ (**3**), then $[(PA)_2Fe^{IV}(O_2)]$ (**7**) and O_2, and (d) O_2 to form an adduct, $[(PA)_2Fe^{III}(O_2)(OOR') + pyH^+]$ (**5**), that reacts with *c*-C_6H_{12} to form *c*-$C_6H_{10}(O)$, [*K*] = 8.2 (*t*-BuOOH) and 2.1 (HOOH). When $PhCH_2CH_3$ or *c*-C_6H_{10} are the substrates (RH), **5** reacts to form $[(PA)_2Fe^{IV}(OH)(OOR)]$ (**6**), which in turn reacts with RH and O_2 in a catalytic cycle to give PhC(O)Me or *c*-$C_6H_8(O)$ [up to 7 O_2 turnovers per iron with $Fe^{II}(OPPh_3)_4^{2+}$]. Species **7** reacts with *cis*-PhCH=CHPh to give PhCH(O).

In a recent report[1] we discussed the activation of excess HOOH and *t*-BuOOH by iron(II) and cobalt(II) complexes for selective reaction with the methylenic-carbon centers of hydrocarbons (RH) to yield ROOR'(H or *t*-Bu) (40–80% efficiency).

$$c\text{-}C_6H_{12} + 2\ R'OOH \xrightarrow{ML_x} c\text{-}C_6H_{11}OOR' + H_2O + R'OH \qquad (1)$$

On the basis of the product profiles and relative reactivities we proposed that the reactive intermediate for the process, $\{L_xFe^{IV}(OH)[OOR']\}$ (**3**), was formed from a one-to-one $Fe^{II}L_x$/HOOR' precursor adduct $[L_xFe^{II}OOR' + BH^+]$ (**1**) that reacts as a Fenton reagent. However, three results have prompted further study and a reconsideration: (a) the kinetic isotope effects [*K*] for *c*-C_6H_{12}/*c*-C_6D_{12} with 5 mM $Fe^{II}(PA)_2$ (PA, picolinate)/100 mM HOOR' are 2.5 (HOOH) and 8.4 (*t*-BuOOH), which is an unreasonably large difference for **3** as the primary reactant; (b) in the absence of O_2 the $Fe^{II}(PA)_2$/*t*-BuOOH system yields as much *c*-$C_6H_{10}(O)$ as *c*-$C_6H_{11}OOBu$-*t*;[1] and (c) in the absence of substrate the various $Fe^{II}L_x$ complexes catalyze the disproportionation of HOOH (rapid) and *t*-BuOOH (slow) to O_2 and R'OH.

Most[2–6] regard Fenton chemistry as synonymous with the *in situ* production of free HO· from the one-to-one combination of iron(II) and HOOH. With this assumption, subsequent reactions have been based on the primary chemistry of HO· (usually generated via pulse radiolysis),[7] which reacts with iron(II) (*k*, 3 x 10^8 $M^{-1}s^{-1}$) and hydrocarbons [CH_4 (*k*, 0.11 x 10^9 $M^{-1}s^{-1}$), C_2H_6 (*k*, 1.8 x 10^9 $M^{-1}s^{-1}$), *c*-C_6H_{12} (*k*, 4.4 x 10^9 $M^{-1}s^{-1}$), and $PhCH_2CH_3$ (*k*, 7.5 x 10^9 $M^{-1}s^{-1}$); 85% aryl addition and 15% H-abstraction]. The resultant carbon radicals (R·) (a) dimerize to R_2, (b) react with a second HO· to form ROH, and (c) in the air, couple with O_2 to form ROO·. The resultant ROO· radicals are unreactive with saturated hydrocarbons and couple to give an unstable intermediate [ROOOOR] that homolytically dissociates to ROOR and O_2.[4]

The $Fe^{II}(PA)_2$ complex in combination with HOOH in 2:1 py/HOAc is an effective Fenton reagent for organic substrates,[2] and has reactivities and product profiles that are closely similar to those for traditional aqueous Fenton reagents.[8] The primary step is nucleophilic addition, e.g.,

$$Fe^{II}(PA)_2 + HOOH \underset{(py)_2HOAc}{\overset{k,\ 2\times10^3\ M^{-1}s^{-1}}{\rightleftharpoons}} \underset{\mathbf{1}}{[(PA)_2Fe^{II}OOH + pyH^+]} \xrightarrow{c\text{-}C_6H_{12}} (c\text{-}C_6H_{11})py + Fe^{II}(PA)_2 + 2\,H_2O \quad (2)$$

KIE, 1.7

This Fenton reagent has reactivity ratios (k_A/k_B) [in comparison with free HO·][7] with *c*-C_6H_{12}/*c*-C_6D_{12} (KIE,

kinetic isotope effect) of 1.7 [versus 1.0], with 1°/2°/3° carbon centers (per C–H, normalized) of 0.07/0.44/1.0 [versus 0.41/0.50/1.0], and with c-C_6H_{12}/$PhCH_2CH_3$ of 2.0 [versus 0.6]. Although free HO· reacts with CH_4, Fenton reagents are unreactive.[6,8] When $PhCH_2CH_3$ is the substrate, HO· reacts primarily by aryl addition (85% $HOPh{\cdot}CH_2CH_3$),[7] but Fenton reagents react exclusively with the alkyl side chain.[1] A recent study[9] provides clear kinetic evidence that free HO· is not the dominant reactant from 1:1 combinations of iron(II) complexes and HOOH, but rather the nucleophilic adduct (**1**, "bound HO·") reacts directly with substrates. All of this is compelling evidence (a) that Fenton reagents do not produce (i) free HO·, (ii) free carbon radicals, or (iii) aryl adducts (HO–Ar·); and (b) that nucleophilic adducts (**1**) are the primary reactant.

Another recent report[10] proposed that a $Fe^{III}Cl_3$/HOOH system initially forms [Fe^{V}=O], which reacts with c-C_6H_{12} (RH) to give [Fe^{V}(OH)(R)]. In the presence of $^{18}O_2$ this system yields c-$C_6H_{10}(^{18}O)$ and c-$C_6H_{11}{}^{18}OH$. A similar incorporation of O_2 into $PhCH_2CH_3$ is induced by a 1:1 combination of $Cu^{I}(bpy)_2^{+}$ and t-BuOOH

$$PhCH_2CH_3 + O_2 \xrightarrow{Cu^{I}(bpy)_2^{+},\ t\text{-BuOOH}} PhC(O)CH_3 + H_2O \qquad (3)$$

with up to 2.4 O_2 turnovers per copper.[11]

A preliminary experiment with $Fe^{II}(PA)_2$ (5 mM)/t-BuOOH (5 mM)/c-C_6H_{12} in a $(py)_2$HOAc solution matrix under argon gave (c-C_6H_{11})py (4 mM, 80% reaction efficiency) as the only detectable product. However, in the presence of O_2 (1 atm, 3.4 mM) the sole product was c-C_6H_{10}(O) (4 mM).

These considerations have prompted a systematic investigation of six iron complexes {$Fe^{II}(PA)_2$, $Fe^{II}(bpy)_2^{2+}$, $Fe^{II}(OPPh_3)_4^{2+}$, $Fe^{II}(MeCN)_4^{2+}$, (Cl_8TPP)-Fe^{II} [Cl_8TPP, tetrakis(2,6-dichlorophenyl)porphyrin], and $Fe^{III}Cl_3$} in combination with t-BuOOH and HOOH to activate O_2 for the oxygenation of hydrocarbons [c-C_6H_{12} $PhCH_2CH_3$, $PhCH(Me)_2$, c-C_6H_{10}, and *cis*-PhCH=CHPh]. In all cases substrate conversions are increased in the presence of O_2, which is incorporated in the products.

Experimental Section

Equipment

The reaction products were separated and identified with a Hewlett-Packard 5880A Series gas chromatograph equipped with an HP-1 capillary column (cross-linked methyl-silicone-gum phase, 12 m x 0.2 mm i.d.) and by gas chromatography-mass spectrometry (Hewlett-Packard 5790A Series gas chromatograph with a mass-selective detector). A Vacuum Atmospheres glovebox was used for the storage, preparation, and addition of air-sensitive and water-sensitive reagents.

A three-electrode potentiostat (Bioanalytical Systems Model CV-27) with a Houston Instruments Model 200 XY recorder was used to record the voltammograms. The experiments were conducted in a 15-mL electrochemical cell with provision to control the presence of dioxygen with an argon-purge system. The working electrode was a Bioanalytical Systems glassy-carbon inlay (area, 0.09 cm^2), the auxiliary electrode a platinum wire, and the reference electrode a Ag/AgCl wire in an aqueous tetramethylammonium chloride solution that was adjusted to give a potential of 0.00 V vs SCE. The latter was contained in a Pyrex tube with a cracked soft-glass tip, which was placed inside a luggin capillary.[12]

Chemicals and reagents

The reagents for the investigations and syntheses were the highest purity commercially available and were used without further purification. Burdick and Jackson "distilled in glass" grade acetonitrile (MeCN, 0.002% H_2O), pyridine (py, 0.007% H_2O), and glacial acetic acid (HOAc, ACS grade, Fisher) were used as solvents. High-purity argon gas was used to deaerate the solutions. All compounds were dried *in vacuo* over $CaSO_4$ for 24 h prior to use. Ferric chloride (anhydrous, 98%), picolinic acid (PAH, 99%), piperidine (pip, 99%), imidazole (imid, 99%), 2,2'-bipyridine (bpy, 99+%), and triphenylphosphine oxide ($OPPh_3$, 98%) were obtained from Aldrich. Ferrous perchlorate (99+%) was obtained from GFS, hydrogen peroxide (50%, in H_2O) and perchloric acid ($HClO_4$, 70%) from Fisher, and t-BuOOH (5.5 M, in 2,2,4-trimethylpentane) from Aldrich. The organic substrates included: cyclohexane (Aldrich, anhydrous, 99+%), cyclohexane-d_{12} (Aldrich, 99.5 atom % D), ethyl benzene (Kodak, 99.8%), cyclohexene (Fisher, 99%), *cis*-stilbene (Aldrich, 97%), and cumene (Aldrich, 99%).

Synthesis of (Me_4N)PA

Tetramethylammonium picolinate [(Me_4N)PA], which was prepared by the neutralization of picolinic acid (PAH) with tetramethylammonium hydroxide pentahydrate in acetonitrile solution, was recrystallized from 95% MeCN/5% MeOH. The hydroscopic product was stored under vacuum.

[$Fe^{II}(MeCN)_4$](ClO_4)$_2$

The [$Fe^{II}(MeCN)_4$](ClO_4)$_2$ complex was prepared by multiple recrystallizations of [$Fe^{II}(H_2O)_6$](ClO_4)$_2$ from MeCN.

Iron(II) bis(picolinate)

Solutions of $Fe^{II}(PA)_2$ were prepared *in situ* by mixing [$Fe^{II}(MeCN)_4$](ClO_4)$_2$ with a stoichiometric ratio of (Me_4N)PA.

Iron(II) bis(2,2'-bipyridine)

The $Fe^{II}(bpy)_2^{2+}$ complex was prepared *in situ* by mixing $[Fe^{II}(MeCN)_4](ClO_4)_2$ in MeCN with a stoichiometric ratio of bipyridine.

Iron(II) tetrakis-(triphenylphosphine oxide)

The $Fe^{II}(OPPh_3)_4^{2+}$complex was prepared *in situ* by mixing $[Fe^{II}(MeCN)_4](ClO_4)_2$ in MeCN with a stoichiometric ratio of the Ph_3PO ligand.

Tetrakis(2,6-dichlorophenyl)porphyrinato iron(II) complexes [$(Cl_8TPP)Fe^{II}L_2$]

The free porphyrin [Cl_8TPPH_2], which was prepared by a modified procedure,[13] was used to synthesize $(Cl_8TPP)Fe^{III}Cl$[14] and $(Cl_8TPP)Fe^{III}OH$.[15] The $(Cl_8TPP)Fe^{II}(py)_2$, $(Cl_8TPP)Fe^{II}(imid)_2$, and $(Cl_8TPP)Fe^{II}(pip)_2$ complexes were prepared by mixing $(Cl_8TPP)Fe^{III}Cl$ and a 100-fold excess of the appropriate base in MeCN under an inert atmosphere, followed by the addition of $NaBH_4$. The precipitate was then filtered and washed with MeCN and diethyl ether, and dried under vacuum.

Methods

The investigations of HOOH and *t*-BuOOH activation by the iron complexes (1–10 mM) used solutions that contained 1.0 M substrate in 5 mL of MeCN, $(MeCN)_4py$, or $(py)_2HOAc$ (mol-ratios). Hydrogen peroxide (50%) or *t*-BuOOH (5.5 M) was injected to give 5–100 mM HOOH(Bu-*t*). After 18 h with constant stirring at room temperature (24±2°C) under Ar or O_2 (0.2 or 1 atm), samples of the reaction solutions were injected into a capillary-column gas chromatograph for analysis. In some cases the reaction was quenched with water, and the product solution was extracted with diethyl ether. Product species were characterized by GC-MS. Reference samples were used to confirm product identifications and to produce standard curves for quantitative assays of the product species.

The kinetic isotope effect [KIE] was determined with a 1:1 cyclohexane/cyclohexane-d_{12} mixture (0.5 M/0.5 M) as the substrate; the k_H/k_D values were calculated from the product ratios of *c*-$C_6H_{10}(O)$/*c*-$C_6D_{10}(O)$, c-$C_6H_{11}OOBu$-*t*/*c*-$C_6D_{11}OOBu$-*t*, (*c*-C_6H_{11})py/(*c*-C_6D_{11})py, and *c*-$C_6H_{11}OH$/ *c*-$C_6D_{11}OH$. The experiments were designed to be limited by HOOH and *t*-BuOOH in order to (a) evaluate reaction efficiency with respect to oxidant and (b) minimize secondary reactions with the primary products.

Results

The reaction efficiencies and product profiles for the activation of hydrogen peroxide (HOOH) or *t*-butylhydroperoxide (*t*-BuOOH) by the (bis-picolinato)iron(II) complex $[Fe^{II}(PA)_2]$ for reaction with cyclohexane (*c*-C_6H_{12}) and ethylbenzene ($PhCH_2Me$) in a pyridine/acetic acid matrix are summarized in Table 1. The mol-ratio of hydroperoxide to metal catalyst ranges from a one-to-one combination to a ratio of 20-to-1. The results are presented for each combination in the absence of molecular oxygen (O_2) as well as in its presence. In the case of HOOH the presence of O_2 has a limited effect on the efficiency of the process, but with *c*-C_6H_{12} in the absence of O_2 the only detectable product is (*c*-C_6H_{11})py. In contrast, with 1 atm O_2 present the sole product is *c*-$C_6H_{10}(O)$. For a one-to-one combination of $Fe^{II}(PA)_2$/*t*-BuOOH with *c*-C_6H_{12} (1 M) in the absence of O_2 the sole product again is (*c*-C_6H_{11})py (1.5 times larger yield than with HOOH). However, with O_2 present the same shift from the pyridine derivative to *c*-$C_6H_{10}(O)$ as the only detected product occurs, but the reaction efficiency is almost doubled.

With a 20-to-1 HOOH/$Fe^{II}(PA)_2$ ratio the reaction efficiency for $PhCH_2Me$ is essentially the same with or without O_2 present. However, with 20-to-1 *t*-BuOOH/-$Fe^{II}(PA)_2$ the dominant product in the absence of O_2 is Ph(Me)CHOOBu-*t* (27 mM), and in the presence of O_2 is PhC(O)Me (126 mM) and less than 1 mM Ph(Me)CHOOBu-*t*.

The results of Table 1 include a listing of reaction efficiency, which is calculated on the basis that the production of one ketone and/or ROOBu-*t* derivative requires two HOOH or *t*-BuOOH molecules. In addition one HOOH or *t*-BuOOH is assumed to be required per (R)py, ROH, or R_2 derivative of the substrate (RH).

Table 1 also includes the kinetic-isotope-effects [KIE] for *c*-C_6H_{12}/*c*-C_6D_{12} in relation to the various products from this substrate. Thus, the [KIE] value for production of (*c*-C_6H_{11})py is 1.7 with HOOH versus 4.6 with *t*-BuOOH. Similarly the production of ketone has a [KIE] value of 2.5 with HOOH versus 7.6 with t-BuOOH (these values shift to 2.1 and 8.2 in the presence of O_2). In the absence of O_2 t-BuOOH also produces *c*-$C_6H_{11}OOBu$-*t*, which has a [KIE] value of 8.4.

Another measure of the influence of C–H bond energies on reaction probabilities is the product ratio per methylenic carbon (CH_2) for $PhCH_2Me$ (ΔH_{DBE}, 85 kcal mol^{-1}) and *c*-C_6H_{12} [(ΔH_{DBE}, 95.5 kcal mol^{-1});[16] {R} = $k_{PhCH_2Me}/(k_{c\text{-}C_6H_{12}}/6)$]. Thus, for the production of the *c*-$C_6H_{11}O$-OBu-*t* via *t*-BuOOH the [KIE] value is 8.4 and the {R} value is 23.

Table 2 summarizes the product profiles for a group of iron complexes under two sets of reaction conditions. The Section A results are for the combination of 5 mM FeL_x and 5 mM *t*-BuOOH with 1 M *c*-C_6H_{12}, and with 1 M $PhCH_2Me$. For each substrate the product profiles are listed in the absence as well as in the presence of O_2. Section B makes a similar comparison with a 5 mM FeL_x/100 mM *t*-BuOOH combination. In every case, the presence of O_2 enhances the overall reaction efficiency and

Table 1. $Fe^{II}(PA)_2$/HOOH(Bu-*t*)induced auto-oxygenation of methylenic carbon in a $(py)_2HOAc$ solvent

			products (mM, ±5%)[a]							
			$c\text{-}C_6H_{12}$ (1 M)				$PhCH_2CH_3$ (1 M)			
$Fe^{II}(PA)_2$ conc(mM)	HOOH(H) t-BuOOH(Bu) (mM)	O_2 conc (mM)	reac effncy,[b] %	$c\text{-}C_6H_{10}(O)$ [KIE][c]	$c\text{-}C_6H_{11}OOBu$ [KIE][c]	$c\text{-}C_6H_{11}py$ [KIE][c]	reac effncy,[b] %	PhC(O)Me {R}[d]	PhCH(Me)OOBu {R}[d]	PhCH(Me)OH {R}[d]
9	9 (H)	0	44	0		4 [1.7]	44	2		0
9	9 (H)	3.4	44	2		0	89	4 {12}		0
9	9 (Bu)	0	67	0	0	6	167	6	0	3[e] {3.0}
9	9 (Bu)	3.4	111	5 [7.3]	0	0	444	20 {24}	0	0
5	5 (Bu)	0	80	0	0	4	400	9	0	2[e] {3.0}
5	5 (Bu)	3.4	160	4 [8.9]	0	0	640	16 {24}	0	0
5	100 (H)	0	58	27 [2.5]		4 [1.7]	52	23 {5.1}		<1[f]
5	100 (H)	3.4	30	15		0	56	27 {11}		2
5	100 (Bu)	0	55	11 [7.6]	7 [8.4]	19 [4.6]	67	6 {3.3}	27 {23}	1[e]
5	100 (Bu)	0.7 (air)	89	40	2	5	126	47 {7.1}	16	0
5	100 (Bu)	3.4	94	46	1	0	253	126 {16}	0.5	0
5	50 (Bu)	0	64	4	5	14	82	6 {9}	14 {17}	1[e]
5	50 (Bu)	3.4	110	27	0.5	0	304	76 {17}	0	0
5	10 (Bu)	0	90	0	0	9	300	13	1	2[e] {1.4}
5	10 (Bu)	3.4	120	6 [8.5]	0	0	480	24 {24}	0	0
10	20 (Bu)	0	80	0	0	16	165	13	2	3[e] {1.1}
10	20 (Bu)	3.4	120	12 [8.2]	0	0	340	34 {17}	0	0

[a]The product solutions were analyzed by capillary-column gas chromatography and GC-MS after a reaction time of 18 h at 24±2°C.
[b]Reaction efficiency; 100% represents one ketone or ROOBu-*t* per two HOOH(Bu-*t*) molecules and/or one Rpy, R_2, or ROH per HOOH(Bu-*t*).
[c][KIE] = $[k_{c\text{-}C_6H_{12}}/k_{c\text{-}C_6D_{12}}]$, kinetic isotope effect.
[d]{R} = $[k_{PhCH_2Me}/(k_{c\text{-}C_6H_{12}}/6)]$, relative reactivity per (CH_2) for $PhCH_2Me$ vs $c\text{-}C_6H_{12}$.
[e]R–R dimer, mM.
[f]Plus 5 mM $HOPhCH_2CH_3$.

Table 2. FeL_x/*t*-BuOOH-Induced auto-oxygenation of *c*-C_6H_{12} (1 M) and $PhCH_2CH_3$ (1 M)

FeL_x/solvent	O_2 conc (mM)	products (mM, ±5%)[a] c-C_6H_{12} reac effncy,[b] %	c-C_6H_{10}(O)	ROOBu	ROH	$PhCH_2CH_3$ reac effncy,[b] %	PhC(O)Me {R}[c]	ROOBu {R}[c]	ROH {R}[c]
A. 5 mM FeL_x/5 mM t-BuOOH									
$Fe^{II}(PA)_2/(py)_2HOAc$	*0*	80	0	0	4[d]	400	9	0	2[e] {3}
$Fe^{II}(PA)_2/(py)_2HOAc$	*3.4*	160	4.0	0	0	640	16 {24}	0	0
$Fe^{II}(bpy)_2^{2+}$/MeCN	*0*	0	0	0	0	204	3.0	0	4
$Fe^{II}(bpy)_2^{2+}$/MeCN	*8.1*	172	4.3	0	0	422	8.5 {12}	0	4
$Fe^{II}(bpy)_2^{2+}/(MeCN)_4py$	*0*	108	2.7	0	0	376	9.4 {21}	0	0
$Fe^{II}(bpy)_2^{2+}/(MeCN)_4py$	*7*	160	4.0	0	0	560	14 {21}	0	0
$Fe^{II}(OPPh_3)_4^{2+}$/MeCN	*0*	0	0	0	0	652	12	1	6
$Fe^{II}(OPPh_3)_4^{2+}$/MeCN	*8.1*	124	3.1	0	0	928	20 {38}	0	7
$Fe^{II}(MeCN)_4^{2+}$/MeCN	*0*	50	0	0.3	1.9	270	4.2	1.6 {32}	1.9 {6}
$Fe^{II}(MeCN)_4^{2+}$/MeCN	*8.1*	14	0.3	0	0.1	512	11	0	2.8
$Fe^{III}Cl_3$/MeCN	*0*	96	1.6	0	1.6[f]	402	4.6	0	6.6, 4.3[f] {41}
$Fe^{III}Cl_3$/MeCN	*8.1*	96	2.4	0	0	1168	23 {58}	0	12
B. 5 mM/100 mM BuOOH									
$Fe(PA)_2/(py)_2HOAc$	*0*	55	11	7	19[d]	67	6 {3.3}	27 {23}	1[e]
$Fe^{II}(PA)_2/(py)_2HOAc$	*3.4*	94	46	1	0	253	126 {16}	0.5	0
$Fe^{II}(bpy)_2^{2+}$/MeCN	*0*	32	7.1	5.4	7.1	74	12 {10}	20 {23}	9.4 {7.9}
$Fe^{II}(bpy)_2^{2+}$/MeCN	*8.1*	60	22	0.7	14	147	62 {17}	1.1	20 {8.6}
$Fe^{II}(bpy)_2^{2+}/(MeCN)_4py$	*0*	43	7.4	11	1.4, 4.4[d]	83	13 {10}	27 {15}	3.0 {3.3}
$Fe^{II}(bpy)_2^{2+}/(MeCN)_4py$	*7*	109	51	0.6	7.0	216	108 {13}	0	0
$Fe^{II}(OPPh_3)_4^{2+}$/MeCN	*0*	30	5.4	5.7	7.7	72	6.9 {7.7}	27 {28}	4.6 {3.6}
$Fe^{II}(OPPh_3)_4^{2+}$/MeCN	*8.1*	39	13	0	13	225	98 {45}	1.0	28 {13}
$Fe^{II}(OPPh_3)_4^{2+}/(MeCN)_4py$	*0*	46	8.2	11	1.6, 5.9[d]	48	5.7 {4.2}	19 {10}	0
$Fe^{II}(OPPh_3)_4^{2+}/(MeCN)_4py$	*7*	79	37	0	5.6	222	110 {18}	0.6	0
$Fe^{II}(MeCN)_4^{2+}$/MeCN	*0*	22	4.5	2.6	7.4	59	12 {16}	14 {32}	5.9 {4.8}
$Fe^{II}(MeCN)_4^{2+}$/MeCN	*8.1*	31	9.5	0.4	11.3	116	50 {32}	0.7 {10}	14 {7.6}
$(Cl_8TPP)Fe^{II}(py)_2$/MeCN[g]	*0*	28	8.5	3.9	7.3	42	6.8 {4.8}	27 {42}	1
$(Cl_8TPP)Fe^{II}(py)_2$/MeCN[g]	*8.1*	32	13	0	6.4	112	55 {25}	0.4	1
$Fe^{III}Cl_3$/MeCN	*0*	26	4.3	1.9	7.6, 5.9[f]	73	10 {14}	15 {47}	13, 9.2[f] {10}
$Fe^{III}Cl_3$/MeCN	*8.1*	45	15.	0.6	13	209	85 {34}	1.3	37 {17}
$Fe^{III}Cl_3/(MeCN)_4py$	*0*	63	19	5.7	2.5, 11.4[f]	81	10 {3.2}	24 {25}	3.3, 9.6[f] {5.6}
$Fe^{III}Cl_3/(MeCN)_4py$	*7*	94	44	0.5	5.2	302	151 {21}	0	0

[a]The product solutions were analyzed by capillary column gas chromatography and GC-MS after a reaction time of 18 h at 24±2°C.
[b]Reaction efficiency 100% represents one ketone or ROOBu-*t* per two *t*-BuOOH molecules and/or one Rpy or ROH per *t*-BuOOH.
[c]{R}=[$k_{PhCH_2CH_3}/k_{c\text{-}C_6H_{12}}$/6)].
[d]*c*-C_6H_{11}py product, mM.
[e]R–R dimer, mM.
[f]R–Cl product, mM.
[g]1 mM; Cl_8TPP = tetrakis(2,6-dichlorophenyl)porphyrin.

shifts the product profiles from ROOBu-*t* and R(py) derivatives to ketone production. Of all the catalysts, the $Fe^{II}(bpy)_2^{2+}$ complex is the most efficient for the ketonization of *c*-C_6H_{12} (172%, product per two *t*-BuOOH), and $Fe^{III}Cl_3$ is the most efficient for the ketonization of $PhCH_2Me$ (1168%; 4.6 PhC(O)Me per $Fe^{III}Cl_3$/*t*-BuOOH). The $Fe^{II}(OPPh_3)_4^{2+}$ complex is almost as efficient with 4.0 PhC(O)Me per catalyst. The various FeL_x (10 mM)/*t*-BuOOH (20 mM) systems have been evaluated in terms of their efficiencies and product profiles for four hydrocarbon substrates (*c*-C_6H_{12}, $PhCH_2Me$, *c*-C_6H_{10}, and *cis*-PhCH=CHPh); the results are summarized in Table 3.

Four of the catalysts have been further evaluated in terms of their efficiency and selectivity for the auto-oxygenation of cumene [$PhCH(Me)_2$]. The reaction efficiencies and product profiles are summarized in Table 4. The presence of O_2 enhances the reaction efficiency by a factor of 12 in the case of the $Fe^{II}(PA)_2$. However, the ratio of ketone to alcohol with this catalyst is 0.65 whereas in the case of $Fe^{III}Cl_3$ the ratio is 8.6. The $Fe^{II}(OPPh_3)_4^{2+}$ complex is particularly impressive in its ability to activate the *t*-BuOOH/O_2 combination for reaction with $PhCH(Me)_2$. Thus, with O_2 the yield of ketone is enhanced by a factor of 33, the yield of alcohol is enhanced by a factor of 7, and the production of $Ph(Me)C=CH_2$ is increased by a factor of 2.6.

O_2 Activation

The striking feature of the results in Tables 1–4 is the impact of O_2 on the reaction efficiencies and product profiles for the FeL_x/HOOH(Bu-*t*) systems. With 9 mM $Fe^{II}(PA)_2$/9 mM HOOH and 1 M *c*-C_6H_{12} under argon the sole product is 4 mM (*c*-C_6H_{11})py, but under O_2 (1 atm, 3.4 mM) is 2 mM *c*-C_6H_{10}(O). When *t*-BuOOH is used in place of HOOH under argon, the sole product is also 6 mM (*c*-C_6H_{11})py [67% reaction efficiency (product per *t*-BuOOH)], but under O_2 the sole product is 5 mM *c*-C_6H_{10}(O) [111% reaction efficiency (product per two *t*-BuOOH); [KIE] value 7.3]. With 1 M $PhCH_2CH_3$ the reaction efficiency under argon (167%) increases to 444% under O_2, with PhC(O)Me the only product. In the absence of O_2 the latter system produces R–R dimer rather than R–py (from *c*-C_6H_{12}); the relative reactivity per CH_2 group of $PhCH_2Me$ versus *c*-C_6H_{12}, {R}, is 6. In the presence of O_2 the {R} value is 24 for the production of ketone (with HOOH/O_2 the {R} value is 12). All of the complexes exhibit enhanced efficiency and selectivity to produce ketone via O_2 activation, especially for CH_2 groups with weak C–H bonds [e.g., $PhCH_2Me$ (ΔH_{DBE}, 85 kcal mol^{-1}) and *c*-C_6H_{10} (87 kcal mol^{-1})].[16]

Characterization of the reactive intermediates for the $Fe^{II}(PA)_2$/t-BuOOH system

Figure 1 illustrates the cyclic voltammograms in $(py)_2HOAc$ for $Fe^{II}(PA)_2$ in combination with an equal molar quantity of *t*-BuOOH. For such conditions the catalyst is almost immediately converted to the iron(III) valence state. In contrast when O_2 is present the electrochemistry indicates that neither $Fe^{II}(PA)_2$ or its oxidized form is present (curve C, Figure 1). Two minutes after mixing the initial reduction peak (-0.1 V vs SCE) is an irreversible two-electron-per-iron process, and there is no oxidation peak for an initial positive voltage scan.

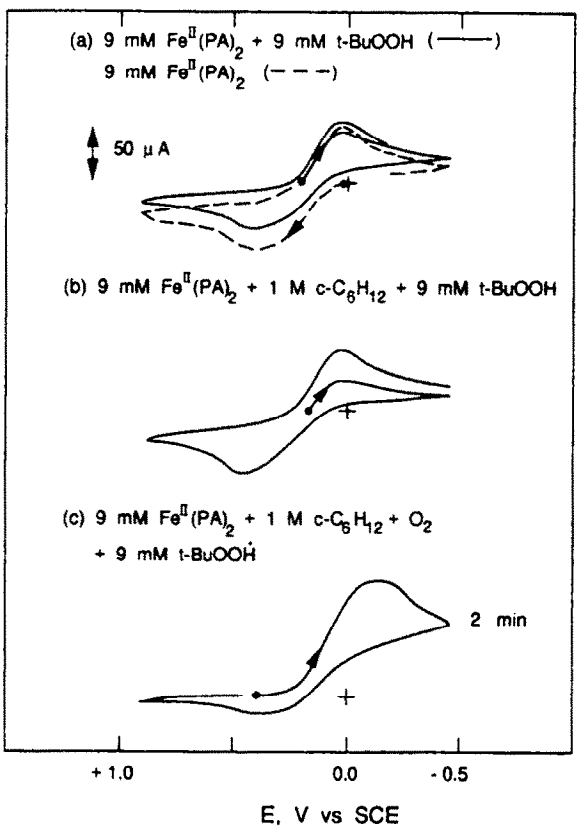

Figure 1. Cyclic voltammograms in $(py)_2HOAc$ [0.1 M $(Et_4N)ClO_4$]for (a) 9 mM $Fe^{II}(PA)_2$ and a combination of 9 mM $Fe^{II}(PA)_2$ and 9 mM *t*-BuOOH; (b) the combination of 9 mM $Fe^{II}(PA)_2$, 9 mM *t*-BuOOH, and 1 M *c*-C_6H_{12}; and (c) the combination of solution (b) in the presence of O_2 (1 atm, 3.4 mM) (2 min after mixing). Scan rate, 0.1 V s^{-1}, GCE (0.09 cm^2); SCE vs NHE, +0.242 V

Figure 2 summarizes the product profiles and reduction current that result from the combination of 9 mM $Fe^{II}(PA)_2$/9 mM *t*-BuOOH with 1 M *c*-C_6H_{12}. In the absence of O_2 the sole product is (*c*-C_6H_{11})py and the reaction is complete within the first few minutes. In contrast, when an atmosphere of O_2 is present the dominant product is *c*-C_6H_{10}(O), which continues to be produced for at least 1500 min. For the latter system, the initial reductive peak current (curve C, Figure 1) is about 120 μA (Figure 2). As the catalytic rate of ketonization slows this current decays from an initial two-electron-per-iron process to a one-electron-per-iron reduction (60 μA). Thus, as the iron catalyst becomes converted to its iron(III) form, it ceases to be effective.

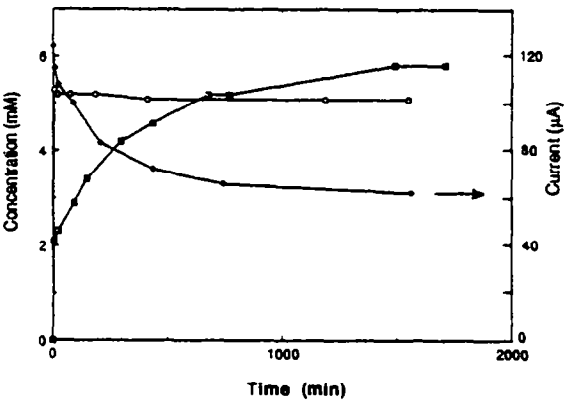

Figure 2. Product profiles and voltammetric reduction currents as function of reaction time for the combination of 9 mM $Fe^{II}(PA)_2$, 9 mM *t*-BuOOH, and 1 M *c*-C_6H_{12} in $(py)_2HOAc$. (A) Under an argon atmosphere: (–o–o–), concentration of (*c*-C_6H_{11})py products. (B) Under an O_2 atmosphere (3.4 mM): (–□–□–), concentration of *c*-$C_6H_{10}(O)$ product; and (–◆–◆–), peak reduction current (-0.1 V vs SCE, Figure 1c)

The cyclic voltammograms of Figure 3 indicate that with a 16-fold excess of *t*-BuOOH relative to $Fe^{II}(PA)_2$ the initial reduction peak is dramatically different from that for a one-to-one combination. In the absence of substrate the current corresponds to approximately five electrons per iron and has a shape commensurate with an electrocatalytic wave with a large excess of a reducible intermediate. When 1 M *c*-C_6H_{12} is present a similar wave is exhibited, but it is only about one half the height (curve b). If the latter system is supplied with excess O_2 the wave is even larger with a current that is indicative of a 10-electron-per-iron catalytic cycle (curve c).

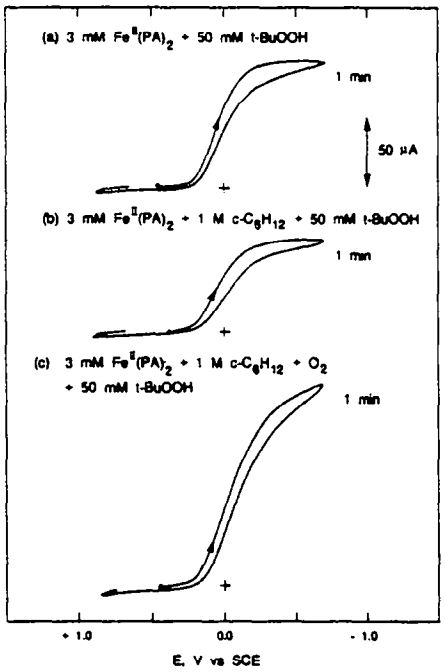

Figure 3. Cyclic voltammograms in $(py)_2HOAc$ [0.1 M $(Et_4N)ClO_4$] for (a) a combination of 3 mM $Fe^{II}(PA)_2$ and 50 mM *t*-BuOOH (one minute after mixing), (b) a combination of 3 mM $Fe^{II}(PA)_2$, 50 mM *t*-BuOOH, and 1 M *c*-C_6H_{12} (one minute after mixing), and (c) the combination of solution (b) in the presence of O_2 (1 atm, 3.4 mM) (one minute after mixing). Scan rate, 0.1 V s^{-1}, GCE (0.09 cm^2); SCE vs NHE, +0.242 V

Additional perspective of these catalyst systems is gained from the electrochemical characterization of the $Fe^{II}(OPPh_3)_4^{2+}$/*t*-BuOOH system, which is illustrated in Figure 4. The reduced complex is oxidized and re-reduced at approximately +1 V vs SCE in a process that has currents that are consistent with a one-electron process. In the presence of an equal molar quantity of *t*-BuOOH the initial oxidation peak decreases with time and has a current intensity approximately one-half of the initial value within eight minutes after mixing. However, the initial irreversible reduction peak (within 1 min of mixing) occurs at -0.2 V vs SCE and has a peak-current that is consistent with a two electron-per-iron process [probably due to the reduction of the *t*-BuOOH adduct of $Fe^{II}(OPPh_3)_4^{2+}$]. The latter system also gives some evidence that there is a slow decomposition of the *t*-BuOOH to yield some O_2 (reduction peak at -0.3 V). This is particularly noticeable for curve c of Figure 4, which indicates that within an eight-minute time period the combination of $Fe^{II}(OPPh_3)_4^{2+}$, *t*-BuOOH, and O_2 yields a system in which neither valence state of the free complex is present to a major extent. In fact, most of it is associated with dioxygen to give a major reduction peak at -0.2 V. When 1 M *c*-C_6H_{12} is present the electrochemistry is not significantly altered other than the complete elimination of any anodic current for the system within four minutes of mixing. In the absence of *t*-BuOOH there is no detectable interaction between $Fe^{II}(OPPh_3)_4^{2+}$ and O_2, and there is no observable reaction with *c*-C_6H_{12} in its absence.

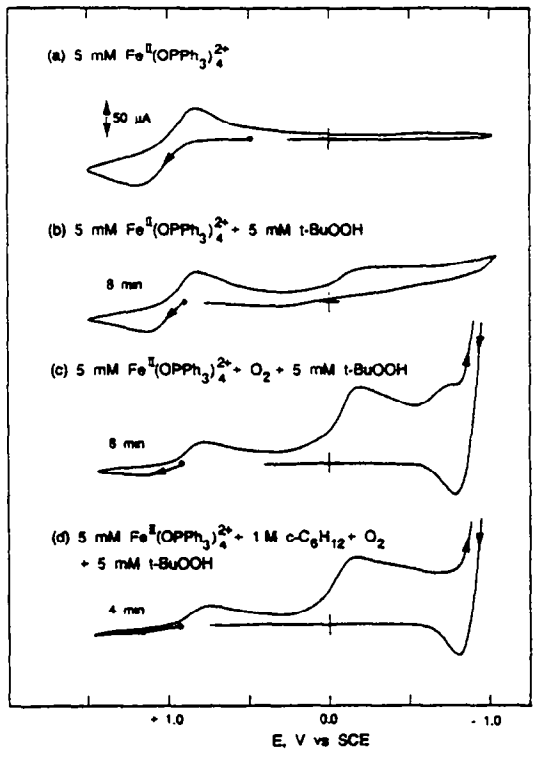

Figure 4. Cyclic voltammograms in MeCN [0.1 M $(Et_4N)ClO_4$] for (a) 5 mM $Fe^{II}(OPPh_3)_4^{2+}$, (b) a combination of 5 mM $Fe^{II}(OPPh_3)_4^{2+}$ and 5 mM *t*-BuOOH (eight minutes after mixing), (c) the combination of solution (b) in the presence of O_2 (1 atm, 8.1 mM) (eight minutes after mixing), and (d) the combination of solution (c) plus 1 M *c*-C_6H_{12} (four minutes after mixing). Scan rate, 0.1 V s^{-1}, GCE (0.09 cm^2); SCE vs NHE, +0.242 V

Table 3. Activation of O_2 by various FeL_x (10 mM)/*t*-BuOOH (20 mM) systems for the oxygenation of several hydrocarbon substrates[a]

		Products (mM ±5%)														
		c-C_6H_{12}				$PhCH_2CH_3$				c-C_6H_{10}				c-PhCH=CHPh (0.6 M)		
FeL_x (10 mM)/solvent (20 mM t-BuOOH)	O_2 conc (mM)	reac[b] effncy %	c-C_6H_{10}(O)	ROOBu	R–OH	reac[b] effncy, %	PhC(O)Me	ROOBu	ROH	reac[b] effncy, %	c-C_6H_8(O)	ROOBu	ROH	reac[b] effncy, %	PhCH(O)	PhC(O)C(O)Ph
$Fe^{II}(PA)_2/(py)_2HOAc$	0	80	0	0	16[c]	169	13	2.3	3.2	35	0	0.9	5.1[d]	18	3.6	0
	3.4	120***	12	0	0	340	34	0	0	466	45	0.5	2.2	152	16	4.9
$Fe^{III}Cl_3/MeCN$	0	0	0	0	0	57	2.9	0	5.5	56	0	2.1	6.9	24	2.3	0.8
	8.1	69*	4.8	0	4.2	206	16	0	9.2	1060**	71	0.5	69	120*	19	1.6
$Fe^{III}Cl_3/(MeCN)_4py$	0	35	0	0.4	6.1[c]	101	5.0	3.4								2.3,1.0[d]
	7	100**	10	0	0	300	30	0								0
$Fe^{II}(bpy)_2^{2+}/MeCN$	0	20	0	2.0	0	68	2.7	1.9	3.4,0.5[d]	53	0	4.1	2.5	25	2.0	1.0
	8.1	62	3.7	0	4.9	405**	35	0	11	1178***	86	1.8	60	139**	21	2.2
$Fe^{II}(bpy)_2^{2+}/(MeCN)_4py$	0	36	0	0	7.1[c]	70	5.0	0.6								1.4[d]
	7	22	2.2	0	0	189	18	0								1.7
$Fe^{II}(OPPh_3)_4^{2+}/MeCN$	0	21	0	0.9	2.3	80	3.6	3.7								1.3
	8.1	27	1.8	0.1	1.6	205	19	0.1								2.7
$Fe^{II}(OPPh_3)_4^{2+}/(MeCN)_4py$	0	48	0	0	9.6[c]	103	0	0.8	4.9,1.4[d]	52	0	0	4.2,6.2[d]	8	1.6	0
	8.1	69	4.3	0	6.1	460***	38	0	16	792*	60	0.5	35,2.5[d]	261***	45	2.4
$Fe^{II}(MeCN)_4^{2+}/MeCN$	0	42	0	0	8.5[c]	117	4.1	0.9	1.5,1.2[d]							
	7	36	3.6	0	0	380	38	0	0							

[a]The product solutions were analyzed by capillary-column gas chromatography and GC-MS after a reaction-time of 18 h at 24±2°C.
[b]Reaction efficiency; 100% represents one ketone or ROOBu-*t* per two HOOH(Bu-*t*) molecules and/or one Rpy or ROH per HOOH(Bu-*t*) (***), (**), and (*) represent the most, second most, and third most efficient systems for the production of the primary production of the primary product.
[c]*c*-C_6H_{11}py product, mM.
[d]R–R dimer, mM.
[e]R–Cl product, mM.

Table 4. FeL_x /*t*-BuOOH -Induced auto-oxygenation of cumene [$PhCH(Me)_2$, 1 M]

FeL_x/solvent (10 mM)/(20 mM t-BuOOH)	O_2 conc (mM)	reac effncy,[b] %	products (mM ±5%)[a] PhC(O)Me	$Ph(Me)_2COH$	$Ph(Me)C=CH_2$	$Ph(Me)_2COOBu\text{-}t$
$Fe^{II}(PA)_2/(py)_2HOAc$	*0*	54	1.2	1.4	7.0	0
$Fe^{II}(PA)_2/(py)_2HOAc$	*3.4*	661	37	57	1.9	0
$Fe^{II}(bpy)_2^{2+}$/MeCN	*0*	81	1.4	5.0	6.7	0.8
$Fe^{II}(bpy)_2^{2+}$/MeCN	*8.1*	218	9.4	12	10	1.4
$Fe^{II}(OPPh_3)_4^{2+}$/MeCN	*0*	75	1.4	2.4	9.7	0
$Fe^{II}(OPPh_3)_4^{2+}$/MeCN	*8.1*	670	46	17	25	0
$Fe^{III}Cl_3$/MeCN	*0*	76	1.6	2.1	8.5	0.7
$Fe^{III}Cl_3$/MeCN	*8.1*	297	19	2.2	18	0.6

[a]The product solutions were analyzed by capillary-column gas chromatography after a reaction-time of 18 h at 24±2°C.
[b]Reaction efficiency; 100% represents one ketone or ROOBu-*t* per two *t*-BuOOH molecules and/or one ROH or $Ph(Me)C\text{-}CH_2$ per *t*-BuOOH.

The combination of $Fe^{II}(OPPh_3)_4^{2+}$ with excess HOOH in MeCN results in the rapid evolution of O_2 and the autoxidation of the iron complex to approximately equal amounts of $(Ph_3PO)_4^{2+}Fe^{III}OH$ and $(Ph_3PO)_4^{2+}Fe^{III}OOH$ [λ_{max}, 576 nm (ϵ 1700 $M^{-1}cm^{-1}$)].[17] Combination of two $Fe^{III}(OPPh_3)_4^{3+}$ molecules per HOOH in MeCN results in their rapid reduction and the evolution of O_2, which also occurs with a 2-to-1 combination of $Fe^{III}Cl_3$ and HOOH.

Discussion and Conclusions

Elementary reactions

The results of Tables 1–3 and Figure 1 confirm that the primary chemistry for these systems is nucleophilic addition by HOOH(Bu-*t*) to the iron complex,[1,8,9,11,18] e.g.,

$$Fe^{II}(PA)_2 + HOOH(Bu\text{-}t) \underset{}{\overset{py}{\rightleftharpoons}} \underset{1}{[(PA)_2Fe^{II}OOH(Bu\text{-}t)} + pyH^+] \quad (4)$$

With one-to-one stoichiometry and in the absence of substrate and O_2 the adduct (**1**) reacts with the iron(II) complex via a Fenton process

$$1 + Fe^{II}(PA)_2 \xrightarrow{k} 2\ (PA)_2Fe^{III}OH(Bu\text{-}t) \quad (5)$$

With HOOH in a $(py)_2HOAc$ matrix the apparent second-order rate constant, k, has a value of 2×10^3 $M^{-1}s^{-1}$.[18]

In the presence of 1 M c-C_6H_{12} species **1** [from the 1:1 combination of $Fe^{II}(PA)_2$ and HOOH] reacts via a Fenton process to give an intermediate (**2**) that produces 2-(c-C_6H_{11})py and 4-(c-C_6H_{11})py

$$1 + c\text{-}C_6H_{12} \xrightarrow{py} \underset{2}{[(PA)_2Fe^{IV}(OH)[py(c\text{-}C_6H_{11})]} \longrightarrow Fe^{II}(PA)_2 + \underset{(c\text{-}C_6H_{11})py + H_2O}{} \quad (6)$$

With 9 mM $Fe^{II}(PA)_2$ the process is 44% efficient and has a kinetic-isotope-effect [KIE] with c-C_6H_{12}/c-C_6D_{12} of 1.7 (Table 1).[18] Via the use of PhSeSePh as a trapping agent the process of eq. 6 becomes 100% efficient with 93% of the product c-C_6H_{11}SePh.[8] When 9 mM t-BuOOH is used in place of HOOH the process is 67% efficient with a [KIE] value of 4.6 (Table 1).[18]

The combination of a 20-fold excess of HOOH(Bu-*t*) with $Fe^{II}(PA)_2$ in the absence of substrate results in its catalytic disproportionation (rapid in the case of HOOH and slow in the case of t-BuOOH; see Figure 3)

$$1 + HOOH(Bu\text{-}t) \longrightarrow \underset{3}{[(PA)_2Fe^{IV}(OH)(OOH(Bu\text{-}t))]} \longrightarrow \underset{7}{[(PA)_2Fe^{IV}(O_2)]} \longrightarrow Fe^{II}(PA)_2 + O_2 \quad (7)$$
$$\text{HOH(Bu)} \qquad\qquad \text{HOH(Bu)}$$

With 1 M c-C_6H_{12} present under an argon atmosphere the 5 mM $Fe^{II}(PA)_2$/100 mM HOOH system yields 27 mM c-$C_6H_{10}(O)$ and 4 mM (c-C_6H_{11})py (the respective [KIE]-values are 2.5 and 1.7). However, almost half of the HOOH is decomposed to O_2 (eq. 7 and Table 1). When t-BuOOH is used in place of HOOH the system yields 7 mM c-$C_6H_{11}OOBu\text{-}t$ ([KIE] = 8.4), 11 mM c-$C_6H_{10}(O)$ ([KIE] = 7.6), and 19 mM (c-C_6H_{11})py ([KIE] = 4.6). Again, almost half the t-BuOOH is decomposed to O_2 via eq. 7.

Although we have previously proposed that species **3** (eq. 7) reacts with c-C_6H_{12} to form c-$C_6H_{11}OOH(Bu\text{-}t)$, the present results make this an unreasonable proposition.[1] If species **3** were the reactive intermediate for the production of c-$C_6H_{11}OOH(Bu\text{-}t)$ the respective [KIE] values for HOOH and t-BuOOH should be closely similar (rather than 2.5 and 7.6). The present results [as well as those for the $Cu^I(bpy)_2^+$ system][11] are more consistent with a path that has species **2** (eq. 6) as the precursor intermediate, which reacts with excess HOOH or t-BuOOH {the respective [KIE] values for formation of c-$C_6H_{11}OOH(Bu\text{-}t)$ are about 1.5-times as large as those for formation of species **2**}

$$2 + HOOH(Bu\text{-}t) \longrightarrow \underset{4}{[(PA)_2Fe^{IV}[OOH(Bu)][py(c\text{-}C_6H_{11})]} \longrightarrow Fe^{II}(PA)_2 + c\text{-}C_6H_{11}OOH(Bu\text{-}t) \quad (8)$$
$$H_2O$$

A similar proposal of a nucleophilic-substitution (S_N2) reaction on an intermediate has been presented recently for a $Fe^{III}(NO_3)_3$/HOOH(Bu-*t*)/c-C_8H_{16}, c-C_6H_{12} system ([KIE] value for HOOH, 2.2, and for t-BuOOH, 8.0).[19]

Activation of dioxygen (O_2)

The 9 mM $Fe^{II}(PA)_2$/9 mM t-BuOOH system in the absence of O_2 and substrate, reacts via a Fenton process (eq. 5) to give $(PA)_2Fe^{III}OH(Bu\text{-}t)$ (curve a, Figure 1). However, the presence of 1 M c-C_6H_{12} causes it to compete with $Fe^{II}(PA)_2$ for reaction with species **1** (eq. 4) to give species **2** (eq. 6). In the presence of O_2 (with or without 1 M c-C_6H_{12}) there is no evidence for free $Fe^{II}(PA)_2$ in the reaction matrix; but only a new two-electron irreversible reduction wave (curve c, Figure 1). With c-C_6H_{12} present the peak current decreases with the time of reaction to about 50% of its initial value, which correlates with the rate of production of c-$C_6H_{10}(O)$ (Figure 2). These observations are compelling evidence that species **1** (formed from t-BuOOH) binds O_2 to form **5**

$$1 + O_2 \longrightarrow \underset{5}{[(PA)_2Fe^{III}(OOBu\text{-}t)(O_2)} + pyH^+] \quad (9)$$

which reacts with excess c-C_6H_{12} to produce c-$C_6H_{10}(O)$ (Table 1)

$$5 + c\text{-}C_6H_{12} \longrightarrow \underset{6}{[(PA)_2Fe^{IV}(OOC_6H_{11})(OH)]} \xrightarrow{c\text{-}C_6H_{12}} Fe^{II}(PA)_2 + c\text{-}C_6H_{10}(O) + c\text{-}C_6H_{11}OH + H_2O \quad (10)$$
$$t\text{-BuOH}$$

With pyridine-containing systems most of the alcohol product (eq. 10) becomes a substrate to **5** and **6** to give ketone (Tables 2 and 3). The dioxygen adduct (**5**) appears to be the steady state primary reactive intermediate rather than species **1** on the basis of (a) the enhanced [KIE] and {R} values for ketone formation {8.7 vs 4.6 [for formation of (c-C_6H_{11})py] and 16 vs 3 [for formation of (R)py, R–R, or ROH], respectively; Table 1} and (b) the electrochemical results of Figures 1 and 2. The latter indicate (a) that an O_2-adduct (**5**) is formed with or without substrate present, (b) that product is produced at a rate that is proportional to the concentration of **5**, and (c) that the system ceases to be reactive when **5** is transformed to $(PA)_2Fe^{III}OH(Bu\text{-}t)$. The electrochemical reduction of **5** yields HOOH,

$$5 + 2e^- + HOAc \longrightarrow \underset{1}{(PA)_2Fe^{II}OOBu\text{-}t} + HOOH + AcO^- + py \quad (11)$$

which reacts with **1** via eq. 7.

The production of 16 mM PhC(O)Me by the 5 mM $Fe^{II}(PA)_2$/5 mM t-BuOOH/O_2/1 M $PhCH_2CH_3$ system (Table 1) indicates that (a) most of the oxygen in the product comes from O_2 and (b) the reaction is initiated by species **5** (eq. 9) via eq. 10, but (c) the catalytic cycle is carried by species **6** (three times as much product as initial t-BuOOH)

$$\underset{6}{\{(PA)_2Fe^{IV}[OOCH(Me)Ph]\}(OH)} + PhCH_2CH_3 + O_2 \longrightarrow 6 + PhC(O)Me + H_2O \quad (12)$$

Cyclohexene (c-C_6H_{10}) has similar reactivity with at least 2.5 O_2 turnovers per $Fe^{II}(PA)_2$ via eq. 12 (Table 3).

The product profiles for cumene [$PhCH(Me)_2$, Table 4] are unique for each of the catalysts. With the $Fe^{II}(PA)_2/t$-BuOOH system, the presence of O_2 enhances the reaction efficiency by a factor of 12, and shifts the product profile from $Ph(Me)C{=}CH_2$ as the dominant species to Ph(Me)COH and PhC(O)Me. In the absence of O_2, species **1** produces $Ph(Me)C{=}CH_2$

$$PhCH(Me)_2 + 1 \longrightarrow Ph(Me)C{=}CH_2 + Fe^{II}(PA)_2 + H_2O + t\text{-BuOH} \quad (13)$$

However, with O_2 present species **5** is formed to react with $PhCH(Me)_2$ via eq. 10 to give **6**, which can collapse to give PhC(O)Me

$$\underset{6}{\{(PA)_2Fe^{IV}(OH)[OOC(Me)_2Ph]\}} \longrightarrow PhC(O)Me + H_2C(O) + Fe^{II}(PA)_2 + H_2O \quad (14)$$

The product profile of Table 4 indicates that species **6** becomes a catalyst for the further oxygenation of $PhCH(Me)_2$ to give $Ph(Me)_2COH$ as the dominant product.

$$2\,PhCH(Me)_2 + 2\,O_2 \xrightarrow{6} PhC(O)Me + Ph(Me)_2COH + H_2C(O) + H_2O \quad (15a)$$

$$2\,PhCH(Me)_2 + O_2 \xrightarrow{6} 2\,Ph(Me)_2COH \quad (15b)$$

In contrast, with $Fe^{II}(OPPh_3)_4^{2+}$ the dominant products are PhC(O)Me and $Ph(Me)C{=}CH_2$, and with $Fe^{III}Cl_3$ equal amounts of PhC(O)Me and $Ph(Me)C{=}CH_2$ are produced.

The dioxygenation of *cis*-PhCH=CHPh by the $Fe^{II}(PA)_2/t$-BuOOH system (Table 3) is enhanced by a factor of five in the presence of O_2. Apparently species **5** (eq. 9) is a reactive intermediate for such substrates and thereby catalyzes the O_2/substrate reaction

$$cis\text{-}PhCH{=}CHPh + O_2 \xrightarrow{5} 2\,PhCH(O) \quad (16)$$

With 20:1 $HOOH(Bu\text{-}t)/Fe^{II}(PA)_2$ ratios, substantial fractions of the $HOOH(Bu\text{-}t)$ are decomposed to O_2 via species **3** (eq. 5) (rapidly for HOOH and slowly for t-BuOOH). This internally generated O_2 in turn combines with **1** to form **5** (eq. 9), which accounts for the production of ketone (rather than $ROOBu\text{-}t$) in O_2-free systems of t-BuOOH.

The electrochemical results of Figure 3 confirm that excess t-BuOOH with $Fe^{II}(PA)_2$ undergoes a sustained disproportionation to O_2 and formation of **5** [same reduction peak as for 1:1 $Fe^{II}(PA)_2/t$-BuOOH in the presence of O_2, Figure 1]. A similar set of observations and rationalizations has been presented for the incorporation of O_2 derived from t-BuOOH in a Fe(III)/t-BuOOH/c-C_8H_{16}/(10:1 py/HOAc) system.[19]

With *cis*-PhCH=CHPh as the substrate, the dominant product is PhCH(O) from a dioxygenation process (Table 3) that is facilitated via species **5** and species **7** (eq. 7)

$$\{(PA)_2Fe^{III}[OOH(Bu)](O_2) + pyH^+\} + cis\text{-}PhCH{=}CHPh \longrightarrow 1 + 2\,PhCHO \quad (17)$$

$$[(PA)_2Fe^{IV}(O_2)] + cis\text{-}PhCH{=}CHPh \longrightarrow 2\,PhCH(O) + Fe^{II}(PA)_2 \quad (18)$$

For 5 mM $Fe^{II}(MeCN)_4^{2+}$/100 mM HOOH/1 M *cis*-PhCH=CHPh in MeCN under argon, 36 mM PhCH(O) and O_2 are produced via the apparent *in situ* formation of a dioxygenase intermediate (**7a**)[1,20]

$$Fe^{II}(MeCN)_4^{2+} + 2\,HOOH \xrightarrow[2L]{} \left[L_2{}^{\cdot}(H_2O)_2{}^{\cdot}Fe^{IV}\!\!<\!\!\begin{matrix}O\\O\end{matrix}\right] \xrightarrow{cis\text{-}PhCH{=}CHPh} 2\,PhCH(O) + L_2{}^{\cdot}Fe^{II}(OH_2)_2{}^{\cdot} \quad (19)$$

Scheme IA outlines a set of reaction paths for the $Fe^{II}(PA)_2$/HOOH(Bu-*t*)/O_2/(*c*-C_6H_{12}, $PhCH_2CH_3$) system, which follows from the preceding arguments and the experimental results. The initial nucleophilic addition of HOOH(Bu-*t*) to $Fe^{II}(PA)_2$ yields the primary reactive intermediate (**1**), which reacts with (a) excess $Fe^{II}(PA)_2$ via path A to give $L_2Fe^{III}OH(Bu)$; (b) excess HOOH(Bu-*t*) via path B and species **3** and **7** to give O_2 and HOH(Bu-*t*), (c) 1 M *c*-C_6H_{12} via path C and species **2** to give (*c*-C_6H_{11})py, (d) 1 M *c*-C_6H_{12} and excess HOOBu-*t* via path C and species **4** to give *c*-C_6H_{11}OOBu-*t*, and (e) O_2 via path D to give **5**, which reacts with RH via **6** and paths E (for $PhCH_2CH_3$), F (for *c*-C_6H_{12}), and G to give products. Scheme IB outlines similar pathways for the $Fe^{II}(bpy)_2^{2+}$/HOOH(Bu) system in MeCN, which forms species **1a** to such a limited extent that the 1:1 system is unreactive with *c*-C_6H_{12} in the absence of O_2 (Tables 2 and 3).

Other iron catalysts

All of the iron complexes of the present study undergo an initial nucleophilic addition by HOOH(Bu-*t*) to form an analogue of species **1**. For the $Fe^{II}L_x^{2+}$ complexes in pure MeCN this is a a cationic reactive intermediate [$L_x{}^+Fe^{II}OOH(Bu\text{-}t) + H_3O^+$] (**1a**) that reacts with excess HOOH(Bu) via path H (Scheme IB) to form **3a**, **7a**, and O_2. In the presence of O_2 **1a** forms **5a** via path I which reacts with *c*-C_6H_{12} or $PhCH_2CH_3$ to form **6a**. The latter reacts with substrates in a manner that is anologous to **6** (Section A).

When pyridine is present in the solvent the primary reactant is [$L_x{}^+Fe^{II}OOH(Bu\text{-}t) + pyH^+$] (**1b**), which reacts with aliphatic substrates (RH) to produce (R)py via [$L_x{}^{2+}Fe^{IV}$(pyR)(OH)] (**2b**).

In the case of $Fe^{III}Cl_3$ the initial event appears to be reduction by HOOH(Bu-*t*) to give $Fe^{II}Cl_2$

$$2\ Fe^{III}Cl_3 + HOOH \longrightarrow 2\ Fe^{II}Cl_2 + O_2 + 2\ HCl \qquad (20)$$

which in turn forms [Cl_2-$Fe^{II}OOH(Bu\text{-}t) + H_3O^+$] (**1c**). The latter reacts with *c*-C_6H_{12} and $PhCH_2CH_3$ via [Cl_2Fe^{IV}(OH)(R)] (**2c**) to produce approximately 50:50 mixtures of ROH and RCl (Tables 2 and 3).[1] With HOOH and *c*-C_6H_{12} the [KIE] value for **1c** is 2.9,[1] and with *t*-BuOOH it is 4.3. The porphyrin catalyst, $(Cl_8TPP)Fe^{II}$, reacts with *t*-BuOOH to form [(Cl_8TPP)-Fe^{II}OOBu-*t* + H_3O^+] (**1d**), which reacts with *c*-C_6H_{12} and $PhCH_2CH_3$ via [$(Cl_8TPP)Fe^{IV}$(OH)(R)] (**2d**) to produce ROH ([KIE] = 5.0).

With excess HOOH(Bu-*t*) the primary reactive intermediates (**1**, **1a**, **1b**, **1c**, and **1d**) disproportionate HOOH (rapidly) and *t*-BuOOH (slowly) via path C and species **3** and **7** (Scheme I). For the conditions of excess *t*-BuOOH and substrate (RH) the species **2**, **2a**, **2b**, **2c**, and **2d** form intermediate **4**, which yields ROOBu-*t* (the [KIE] values range from 5.4 to 10.5 and the {R} values range from 11 to 47, Table 5). The reactivity parameters for $[Co^{II}(bpy)_2{}^{2+}]$[1] and $[Cu^{I}(bpy)_2{}^{+}]$[11] are similar and in accord with the proposition that all of these complexes activate HOOH(Bu-*t*) initially via a species **1**, which reacts with hydrocarbon substrates (RH) via path C to form species **2**. In general the reactivity parameters ([KIE] and {R}) have larger values for the path-C step than for the path-D step of Scheme I, which is consistent with a sequential process.

With excess O_2 most of the species **1** form adducts [**1**(O_2) = **5**] via path D that react with substrates (RH) to form species **6**, which, in the case of *c*-C_6H_{12}, reacts initially with excess *c*-C_6H_{12} via path F and finally with excess $Fe^{II}L_x$ via path G (Scheme I). Thus, the various species **1** (Fenton intermediates), via formation of **5**, catalyze the incorporation of O_2 into the ketone and alcohol products [e.g., $Fe^{II}(OPPh_3)_4{}^{2+}$/*t*-BuOOH, O_2/*c*-C_6H_{12}, Tables 2 and 3].

$$2\ c\text{-}C_6H_{12} + O_2 + t\text{-}BuOOH \xrightarrow{Fe^{II}L_x} c\text{-}C_6H_{10}(O) + c\text{-}C_6H_{11}OH + t\text{-}BuOH + H_2O \qquad (21)$$

Recent results[19] for a $Fe^{III}(NO_3)_3$/*t*-BuOOH/$18O_2$/*c*-C_8H_{16} system in acetonitrile establish that the O-atoms in the *c*-C_8H_{14}(O) and *c*-C_8H_{15}OH products are from O_2. This appears to be the case here, and supports the stoichiometry of eq. 21 [1:20 $Fe^{II}L_x$/*t*-BuOOH systems are 13–51% efficient (ketone per *t*-BuOOH, Table 2B) with 2–13 turnovers per $Fe^{II}L_x$].

For substrates with weak C–H bonds in their CH_2 groups ($PhCH_2Me$ and c-C_6H_{10}), species **6** becomes a catalyst via path E (Scheme I) for the activation of O_2,

$$PhCH_2CH_3 + O_2 \xrightarrow[\text{path E}]{6} PhC(O)CH_3 + H_2O \qquad (22)$$

When the reaction efficiency for such substrates is >200% (ketone per two *t*-BuOOH, Tables 2 and 3) the reaction cycle of path E (Scheme I and eq. 22) must occur {turnovers per $Fe^{II}L_x \geq$ (*t*-BuOOH/$Fe^{II}L_x$) [(% reaction efficiency)-200]/200}. Hence, the 5 mM $Fe^{II}(OPPh_3)_4{}^{2+}$/5 mM *t*-BuOOH/$PhCH_2CH_3$ system has at least 3 O_2 turnovers via path E, which is similar to the 2.4 O_2 turnovers per copper for the 5 mM $Cu^{I}(bpy)_2{}^{+}$/10 mM *t*-BuOOH/$PhCH_2CH_3$ system.[11] Likewise, the 10 mM $Fe^{II}(OPPh_3)_4{}^{2+}$/20 mM *t*-BuOOH/*c*-C_6H_{10} system has almost 7 O_2 turnovers per iron catalyst via eq. 22.

Recent experiments[21] confirm that the combination of $Fe^{II}(DPAH)_2$ ($DPAH_2$ = 2,6-dicarboxyl-pyridine) and O_2 in a pyridine/acetic acid solution results in rapid autoxidation to produce HOOH and Fe^{III}(DPA)(DPAH) k_1, 1.8 ± 0.5 $M^{-1}s^{-1}$).[22]

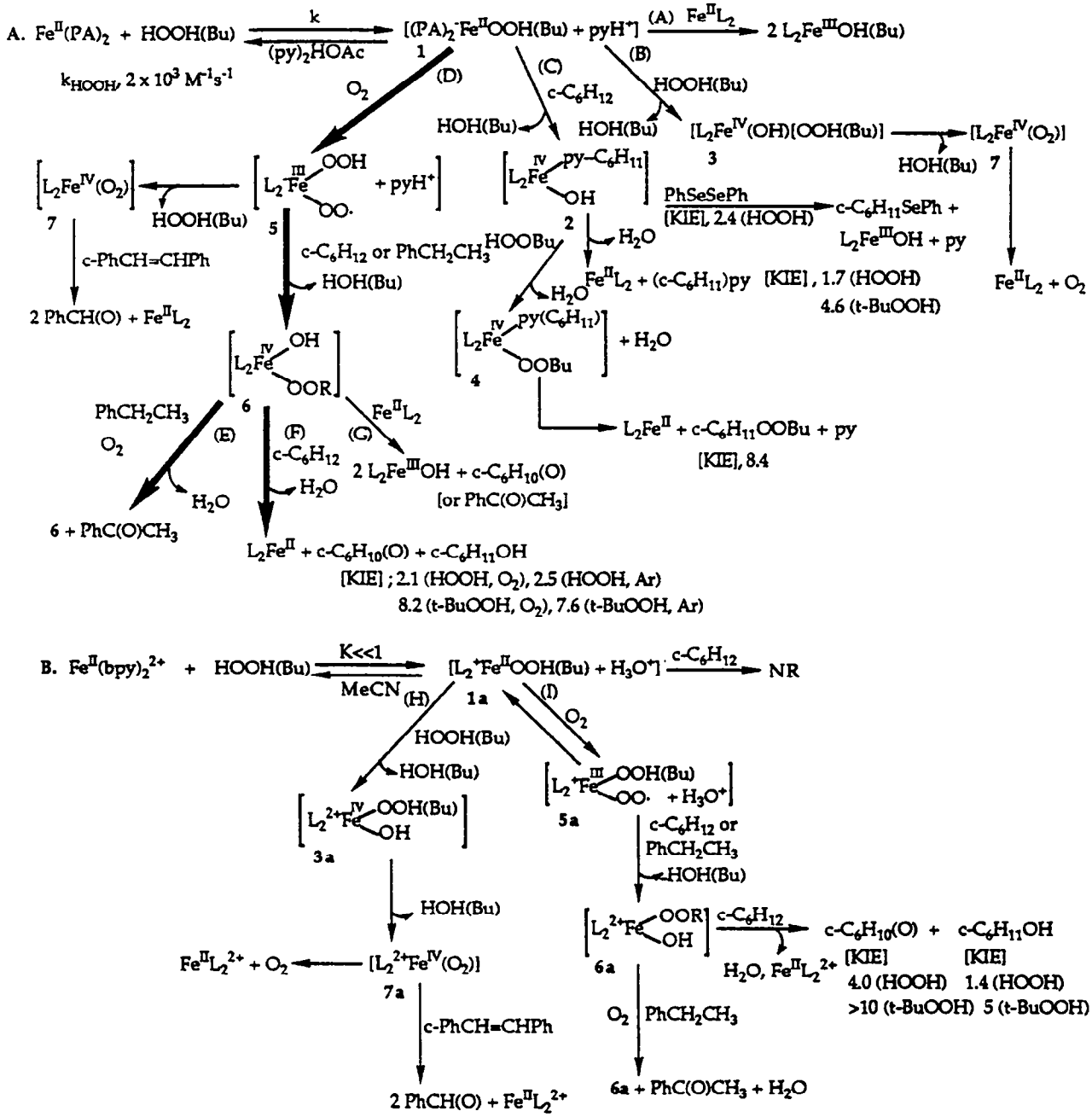

Scheme I. Fenton chemistry and the induced activation of O_2.

Table 5. Reactivity parameters with c-C_6H_{12} and $PhCH_2CH_3$ substrates for various species **1**, **2**, **5**, and **6**

System	HOOH(H) t-BuOOH(Bu)	Species 1 (path C)[b] [KIE]	(R)	Species 2, 4 (path C)[c] [KIE]	(R)	Species 5, 6 (path D)[d] [KIE]	(R)	Species 6 (path D, F)[e] [K]	(R)
$Fe^{II}(PA)_2/py_2HOAc$	H	*1.7*				*2.1*	12		
$Fe^{II}(PA)_2/py_2HOAc$	Bu	*4.6*	3.0	*8.4*	23	*8.2*	16		
$Fe^{II}(OPPh_3)_4^{2+}/MeCN$[f]	H					*>10*		1.9	18
$Fe^{II}(OPPh_3)_4^{2+}/MeCN$	Bu		3.6	*6.4*	28		45		4
$Fe^{II}(bpy)_2^{2+}/MeCN$[f]	H					*4.0*	16	1.4	
$Fe^{II}(bpy)_2^{2+}/MeCN$	Bu			*5.4*	23	*>10*	17	4.8	8
$Fe^{II}(MeCN)_4^{2+}/MeCN$[f]	H					*>10*	27	1.8	
$Fe^{II}(MeCN)_4^{2+}/MeCN$	Bu			*6.0*	32	*>10*	32	5.6	5
$(Cl_8TPP)Fe^{II}(py)_2/MeCN$	Bu	*5.0*	14	*10.5*	42	*10.3*	26		
$Fe^{III}Cl_3/MeCN$[f]	H	*2.9*	2.8			*11*	11		
$Fe^{III}Cl_3/MeCN$	Bu	*4.3*	10	*5.8*	47	*>10*	34		
$Co^{II}(bpy)_2^{2+}/MeCN$[f]	H					*4.0*	16		
$Co^{II}(bpy)_2^{2+}/MeCN$[f]	Bu			*8.7*	58	*9.6*	8	6.3	
$Co^{II}(bpy)_2^{2+}/(MeCN)_4py$[f]	H					*2.9*	6		
$Co^{II}(bpy)_2^{2+}/(MeCN)_4py$[f]	Bu				72				
$Cu^{I}(bpy)_2^{+}/(MeCN)_4py$[g]	H					*2.5*	6	1.4	
$Cu^{I}(bpy)_2^{+}/(MeCN)_4py$[g]	Bu			*7.3*	11	*8.8*	25	>7	

[a] $[K] = [k_{c\text{-}C_6H_{12}}/k_{c\text{-}C_6H_{12}}]$, kinetic isotope effect. $\{R\} = [k_{PhCH_2Me}/(k_{c\text{-}C_6H_{12}}/6)]$, relative reactivity per (CH_2) for $PhCH_2Me$ vs c-C_6H_{12}.
[b] To produce Rpy, ROH, RCl and/or R–R.
[c] To produce ROOBu-*t*.
[d] To produce ketone and ROH from O_2.
[e] To produce ROH from **6**.
[f] Data from Ref. 1.
[g] Data from Ref. 11.

$$Fe^{II}(DPAH)_2 + O_2 \underset{(py)_2HOAc}{\rightleftharpoons} [(DPAH)(DPA)Fe^{III}OOH] \xrightarrow{Fe^{II}(DPAH)_2} HOOH + 2\,Fe^{III}(DPA)(DPAH) \quad (23)$$

The resultant HOOH reacts with excess $Fe^{II}(DPAH)_2$ via nucleophilic addition to give a Fenton reagent [$(DPAH)_2Fe^{II}OOH$ + pyH^+] (**1**) that reacts with excess $Fe^{II}(DPAH)_2$ to give $Fe^{III}(DPA)(DPAH)$ [k_2, (2±1) x 10^3 $M^{-1}s^{-1}$], and in accord with the other paths of Scheme I.

Summary

The one-to-one combination of the $Fe^{II}L_x$ complexes and HOOH(Bu-*t*) yields a species **1** (Scheme I), which reacts as a Fenton reagent with *c*-C_6H_{12} via path C and intermediate **2** to give (*c*-C_6H_{11})py (with HOOH [KIE] = 1.7–2.9 and with *t*-BuOOH [KIE] = 4.3–5.0). In the presence of O_2 the various species **1** form an O_2 adduct (**5**) via path D that reacts with *c*-C_6H_{12} to give intermediate **6**, which reacts via path F to produce *c*-$C_6H_{10}(O)$ (with HOOH [KIE] = 2.1–11 and with *t*-BuOOH [KIE] = 8.2→10) and *c*-$C_6H_{11}OH$ (with HOOH [KIE] = 1.4–1.9 and with *t*-BuOOH [KIE] = 4.8→7). The several species **1** react with excess HOOH (rapidly) and *t*-BuOOH (slowly) via path B (species **3** and **7**) to give O_2, which forms **5** via path D. With excess *t*-BuOOH and *c*-C_6H_{12} in the absence of O_2, the several species **2** undergo nucleophilic substitution via **4** to produce *c*-$C_6H_{11}OOBu$-*t*. Table 5 summarizes these and analogous reactivity parameters for $Co^{II}(bpy)_2^{2+}$ and $Cu^{I}(bpy)_2^{+}$ in relation to the various reaction pathways of Scheme I. Clearly the Fenton chemistry of species **1** does not involve production of free hydroxyl radical (HO·) ([KIE] = 1.0–1.1 for *c*-C_6H_{12}/*c*-C_6D_{12}).[7]

With excess HOOH the various $Fe^{II}L_x$ complexes rapidly disproportionate it via path B to give O_2 and H_2O. Hence, even in the absence of ambient O_2 these systems are never limited in available O_2 for their formation of species **5**. This is in contrast to *t*-BuOOH, which is disproportionated much more slowly and causes its $Fe^{II}L_x$/*t*-BuOOH systems to be limited by available O_2 in their formation of species **5**.

The present results indicate that reduced transition-metal complexes [ML_x; $Fe^{II}L_x$, $Cu^{I}(bpy)_2^{+}$, and $Co^{II}(bpy)_2^{2+}$] undergo nucleophilic addition by hydroperoxides [HOOH(R)] to form [L_xMOOH + BH^+] (**1**), which often binds O_2 to give a species (**5**) that oxygenates hydrocarbons and related organic substrates (Scheme I). Hence, the combination of reduced iron (including heme) and HOOH in a biological matrix almost certainly will lead to the formation of a species **5** with its attendant reactivity.

Acknowledgement

This work was supported by the National Science Foundation under Grant No. CHE-9106742, the Welch Foundation under Grant No. 1042A, and the Monsanto Company with a Grant-in-Aid. We are grateful to Prof. D. H. R. Barton (of this department) for making available preprints of related investigations, and for his assistance and encouragement.

References

1. Tung, H.-C.; Kang, C.; Sawyer, D. T. *J. Am. Chem. Soc.* **1992**, *114*, 3445.

2. Walling, C. *Acc. Chem. Res.* **1975**, *8*, 125.

3. Cohen, G.; Sinet, P. M. In *Chemical and Biochemical Aspects of Superoxide and Superoxide Dismutase*, Vol. 11A, pp. 27–37, Bannister, J. V.; Hill, H. A. O. Eds., Elsevier, New York, 1980.

4. Sheldon, R. A.; Kochi, J. K. *Metal-Catalyzed Oxidations of Organic Compounds*, Chapters 2 and 3, Academic Press, New York, 1981.

5. Stubbe, J.; Kozarich, J. W. *Chem. Rev.* **1987**, *87*, 1107.

6. Rudakov, E. S.; Volkova, L. K.; Tret'yakov, V. P. *React. Kinet. Catal. Lett.* **1981**, *16*, 333.

7. Buxton, G. V.; Greenstock, C. L.; Helman, W. P.; Ross, A. B. *J. Phys. Chem. Ref. Data* **1988**, *17*, 513.

8. Sheu, C.; Sobkowiak, A.; Zhang, L.; Ozbalik, N.; Barton, D. H. R.; Sawyer, D. T. *J. Am. Chem. Soc.* **1989**, *111*, 8030.

9. Yamazaki, I; Piette, L. H. *J. Am. Chem. Soc.* **1991**, *113*, 7588.

10. Barton, D. H. R.; Béviére, S. D.; Chavasiri, W.; Csuhai, E.; Doller, D.; Liu, W.-G. *J. Am. Chem. Soc.* **1992**, *114*, 2147.

11. Sobkowiak, A.; Qiu, A.; Liu, X.; Llobet, A.; Sawyer, D. T. *J. Am. Chem. Soc.* **1993**, *115*, 609.

12. Sawyer, D. T.; Roberts, Jr, J. L. *Experimental Electrochemistry for Chemists*, p. 144, Wiley-Interscience, New York, 1974.

13. Hatano, K.; Safo, M.; Walker, F.; Scheidt, W. *Inorg. Chem.* **1991**, *30*, 1643.

14. Adler, A. D.; Longo, F. R.; Kampas, F.; Kim, J. *J. Inorg. Nucl. Chem.* **1970**, *32*, 2443.

15. Woon, T. C.; Shirazi, A.; Bruice, T. C. *Inorg. Chem.* **1986**, *25*, 3845.

16. Lide, D. R. (Ed.) *CRC Handbook of Chemistry and Physics*, 71st edn, pp. 9, 86, 98, CRC Press, Boca Raton, FL, 1990.

17. Although the latter complex was originally formulated as $[(Ph_3PO)_4(H_2O)Fe^{III}OOFe^{III}(OH_2)(OPPh_3)_4]^{4+}$, current spectroscopic and electrochemical results indicate that it is almost certainly a mononuclear hydroperoxide. Sawyer, D. T.; McDowell, M. S.; Spencer, L.; Tsang, P. K. S. *Inorg. Chem.* **1989**, *28*, 1166.

18. Sheu, C.; Richert, S. A.; Cofré, P.; Ross, Jr, B.; Sobkowiak, A.; Sawyer, D. T.; Kanofsky, J. R. *J. Am. Chem. Soc.* **1990**, *112*, 1936.

19. Barton, D. H. R.; Béviére, S. D.; Chavasiri, W.; Doller, D.; Hu, B. *Tetrahedron Lett.* **1992**, *33*, 5473.

20. Sugimoto, H.; Sawyer, D. T. *J. Am. Chem. Soc.* **1984**, *106*, 4283.

21. Kang, C.; Sobkowiak, A.; Sawyer, D. T. *J. Am. Chem. Soc.*, submitted, November, 1992.

22. Sheu, C.; Sobkowiak, A.; Jeon S.; Sawyer, D. T. *J. Am. Chem. Soc.* **1990**, *112*, 879.